Research Square

Preprints are preliminary reports that have not undergone peer review.
They should not be considered conclusive, used to inform clinical practice,
or referenced by the media as validated information.

Evaluation of Wrapper Fibre Percentage in Lyocell Air-Jet Spun Yarns: Development of a New Method and Analysis of Its Relationship to Yarn Properties

Iva Mertová

iva.mertova@tul.cz

Technical University of Liberec

Eva Moučková

Technical University of Liberec

Petra Jirásková

Technical University of Liberec

Research Article

Keywords: Fibre migration, yarn geometry, helical fibre arrangement, structural parameters, tensile behaviour

Posted Date: November 5th, 2026

DOI: https://doi.org/10.21203/rs.3.rs-10357661/v1

License: This work is licensed under a Creative Commons Attribution 4.0 International License.
Read Full License

Additional Declarations: No competing interests reported.

Evaluation of Wrapper Fibre Percentage in Lyocell Air-Jet Spun Yarns: Development of a New Method and Analysis of Its Relationship to Yarn Properties

Iva Mertová[1*], Eva Moučková[1] 0000-0001-6038-9773, Petra Jirásková[1] 0000-0002-8800-385X

[1]*Technical University of Liberec, Faculty of Textile Engineering, Department of Technologies and Structures, Studentská 2, Liberec, The Czech Republic*

[*] Corresponding author: 0000-0002-3026-8011, iva.mertova@tul.cz

Abstract

Yarn properties are influenced not only by fibre material but also by yarn structure, which is determined by spinning technology and processing conditions. Air-jet spun yarns exhibit a distinctive core-wrapper structure, where a fibre ribbon is helically wrapped around the core. Wrapper fibres significantly influence yarn performance; thus, determining their percentage is essential for modelling yarn behaviour. However, conventional cross-sectional image analysis methods are often inaccurate and subjective. This paper presents a novel method for identifying wrapper and core fibres in air-jet spun yarn, based on which the percentage of wrapper fibres is subsequently calculated. Unlike the subjective approaches proposed in previous studies, this direct method and its modification eliminate subjectivity by classifying fibres into core and wrapper layers using objective, rule-based geometric criteria. The proposed methodology was evaluated using Lyocell air-jet spun yarns spun at three levels of spinning nozzle spacing (the distance between the front roller nip line and the spinning tip inlet). Concurrently, the effects of this parameter on yarn packing density, tenacity, breaking elongation, and hairiness were investigated, alongside the correlation between wrapper fibre percentage and these properties. The results showed a wrapper fibre percentage of approximately 30%, consistent with the literature, with the highest proportion observed at the shortest spinning nozzle spacing. While packing density was not statistically significantly affected, yarn mechanical properties exhibited a non-linear dependence; both tenacity and elongation initially increased with a higher wrapper fibre percentage but decreased after exceeding a critical threshold. Ultimately, a longer spinning nozzle spacing increased yarn tenacity and elongation while decreasing hairiness.

Keywords: Lyocell; Air-jet spinning; Yarn structure; Wrapper fibres; Tensile properties.

Introduction

Lyocell fibre is a new-age regenerated cellulose fibre spun from the solution of wood pulp dissolved in N-methyl morphine oxide. Compared to the previous generation of viscose fibres, Lyocell fibre has better strength, lustre, drapability, and colouring ability (Li et al. 2024). These fibres have a uniform diameter, are thin and flexible, making them suitable for various textile applications (Abdennadher et al. 2016). Lyocell fibres also possess higher fibrillation properties than other cellulose fibres, making them crucial in determining fabrics' surface and comfort properties (Şardağ et al. 2019). Additionally, Lyocell fibres are found to have high moisture absorption and release properties, making them environmentally friendly and suitable for various applications (Kim 2023), mainly in the field of clothing, home textiles, and medical textiles as staple fibres, filaments, staple-spun yarns and products

made of them. In the context of spinning systems, Lyocell fibres have been used in the production of yarn samples to analyse fibre three-dimensional configurations along the axis of low-twist ring spun yarn (Guo and Tao 2016). Fibres have also been blended with cotton to produce ring, compact, and air-jet spun yarns with improved mechanical properties, highlighting their potential for enhancing yarn performance compared to cotton-Promodal yarns (Kılıç and Okur 2010). Studies have also explored the utilisation of Lyocell fibres in the production of compact core-spun yarns, where its properties, such as high comfort features, have been combined with cotton fibres to create yarns with better comfort properties and to analyse the effect of pin-spacer device in drafting system of compact ring spinning machine on yarn and knitted fabrics (Karakan 2019; Vidhya et al. 2021). Also, Lyocell fibres have been spun into yarns on ring, rotor and air-jet spinning machines to compare the properties of knitted fabrics made of these yarns (Pavlović and Vrljičak 2020). The utilisation of Lyocell fibres in staple spun yarn spinning, particularly in air-jet spinning, aims to improve the structural comfort of fabrics.

Air-jet spinning is an essential system in short-staple spinning due to its advantageous production speeds and ability to spun yarns of fine counts (Zeng and Yu 2004). Air-jet spun yarns have lower mass unevenness, less hairiness, higher tensile strength, and lower elongation compared to open-end rotor spun yarns (Erdumlu et al. 2009). Air-jet spun yarn replaces rotor-spun yarn in the clothing sector, especially for knitted fabrics (Ghosh et al. 2005).

During yarn manufacturing on the air-jet spinning machine, the drafting device attenuates an input product, a sliver. Air flow in the nozzle housing transports the fine fibrous strand from the drafting unit to the spinning tip (or hollow spindle) entry. As seen in Fig. 1, the swirling air stream separates some trailing ends of the surface fibres from the fibre bundle and twists them around the yarn body. Leading ends of these fibres converge towards the centre of the yarn and are drawn into the spinning tip (or hollow spindle) by the preceding part of the fibre bundle being formed into yarn (Erdumlu et al. 2012; Stalder 2014). Finally, the winding device takes up the yarn and winds it into the package.

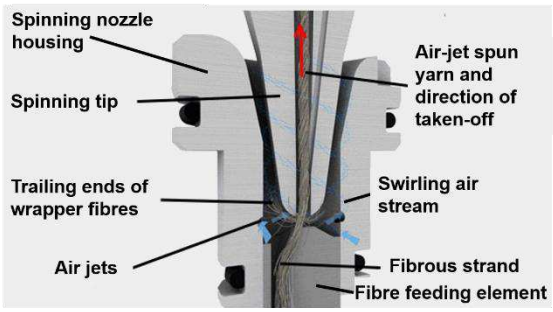


Fig. 1 Principle of yarn formation in the spinning nozzle (adapted and reproduced from Rieter & Textile World 2014 and Mertová and Moučková 2020)

The air-jet spun yarn has a specific, so-called fasciated structure (see Fig. 2), formed of parallel core fibres without twist and sheath (wrapper) fibres of the same type, twisted around the core and holding it together (Basal et al. 2006; Basu 2001).

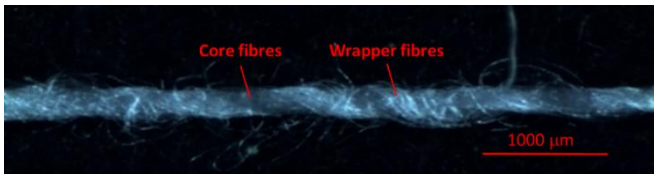


Fig. 2 Longitudinal view of Lyocell air-jet spun yarn

Fibre type, spinning process, and machine variables can influence the specific structure and properties of air-jet-spun yarn. The relationship between fibre properties and machine variables is extensively investigated. However, most scientific articles focus on yarns produced on Murata's MVS machine *(called vortex-spun yarns).* Available studies investigate the influence of nozzle design parameters, processing conditions, and fibre properties on the structure and properties of air-jet spun yarns (for example, Basal and Oxenham 2006; Bhatti et al. 2019; Eldeeb and Demir 2018; Erdumlu and Ozipek 2010; Erdumlu et al. 2012; Kuthalam and Senthilkumar 2014; Lawrence and Baqui 1991). Also, several research works study the mechanics and optimisation of air-jet spinning. For example, studies are focused on the air flow dynamics within the spinning nozzle and spinning tip, the interaction between air currents and fibres, and the effects of process parameters on yarn quality (for example, Eldeeb and Mouckova 2017; Zeng and Yu 2003; Zeng and Yu 2004; Guo et al. 2008). Structural parameters of Vortex spun yarns, such as fibre packing density and fibre distribution in the cross-section, have also been reported (e.g., Zheng et al. 2012; Zou et al. 2014).

Regarding the yarn structure, the twist level and the percentage of wrapper fibres mainly affect the properties of air-jet-spun yarns (e.g., Stalder 2014; Tyagi et al. 2004b). The ratio of wrapper fibres to core fibres was stated to be one of the important aspects of vortex yarn tenacity since wrapper fibres hold the internal parallel fibre bundle tightly together (Başal and Oxenham 2006). According to Shang et al. (2016), the tenacity of viscose vortex spun yarn increases with an increasing number of wrapper fibres and wrapping angle.

The number of wrapper fibres in air-jet spun yarn is influenced by various factors, including the method of determination, yarn count, and specific machine variables. Lower yarn delivery speed results in a slightly lower ratio of wrapper fibres to core fibres, and an increase in both nozzle air pressure and nozzle distance causes a reduction in the ratio of core fibres to wrapper fibres in vortex-spun yarn (Tyagi et al. 2004a). In contrast, Leitner and Schwippl (2015) found that a minimal increase in wrapping fibres was observed with increasing delivery speed on the Rieter air-jet spinning machine. Eldeeb et al. (2017) confirmed that a higher percentage of wrapping fibres in air-jet spun yarn is achieved by setting higher air pressure. Mertová and Moučková (2020) presented that both delivery speed and nozzle air pressure do not influence the frequency ratio of the wrapper fibre in the cross-section of 100 % viscose air-jet spun yarn produced on a Rieter air-jet spinning machine. A value of the ratio of the circumferential speed of machine delivery rollers and the front roller of the drafting device (so-called spinning draft) lower than 1 means a higher percentage of wrapper fibres compared to a spinning draft higher than 1 (Stalder 2014). The next crucial machine variable that impacts the number of wrapper fibres is the distance between the nip point of the top front roller of the drafting device and the tip of the spindle in the vortex spinning systems, so called spinning nozzle spacing (L) (Zou et al. 2009a; Zou et al. 2009b; Tyagi et al. 2004b; Zou et al. 2010; Zou et al. 2008), see Fig. 3. This distance affects yarn parameters and determines the amount of separated free trailing ends of the fibres. If a larger distance L is used, a higher percentage of wrapping fibres is achieved; the yarn has more regular, long wraps and is more resistant to abrasion (Tyagi et al. 2004a; Tyagi et al. 2004b). On the other

hand, however, as the distance *L* increases, the length of the trailing end of the fibres released from the core and rotating in the air vortex increases, resulting in an increase in yarn hairiness (Zou 2009a). Very high distance (higher than fibre length) causes a reduction in vortex spun yarn tenacity (Tyagi et al. 2004a and Tyagi et al. 2004b) due to the increase in the fibre loss rate and a decrease in the number of generated thin places (Zou et al. 2009b). However, according to Tyagi et al. (2004a), if the *L* distance is too small during vortex spinning, the yarn has a lower percentage of wrapping fibres, and its tenacity may not be sufficient for the required application.

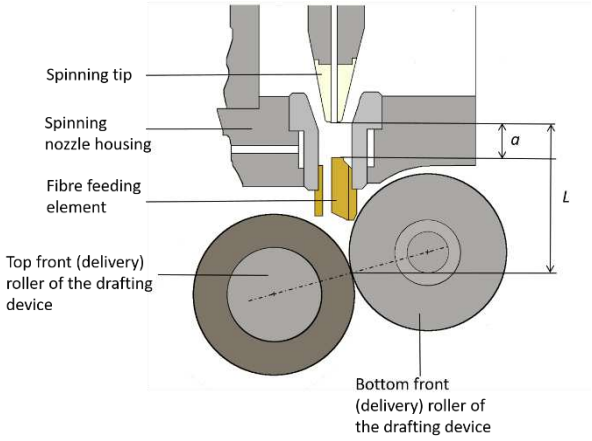


Fig. 3. Schematic illustration of the distance between the nip point of the front rollers of the drafting device and spinning tip inlet (*L*) and the distance between the spinning tip and the fibre feeding element (*a)* of the spinning nozzle (adapted and reproduced from Schaeffler 2007 and Erdumlu et al. 2012)

In the case of the Rieter air-jet spinning machine, the three levels of spinning nozzle spacing (*L*), i.e. distance between the front rollers' nip line and the inlet of the spinning tip, can be chosen. For a given distance *L*, it is necessary to use a different spinning nozzle housing, i.e., a nozzle housing with a different length of the fibre feeding element (shorter distances *L* correspond to shorter fibre feeding elements in the nozzle housing) see Fig. 4.

The fibre feeding element (FFE) is a specially shaped element placed in the nozzle housing at a defined distance before the inlet to the spinning tip (the distance marked as *a* – see Fig. 3). The FFE deflects the fibre strand trajectory away from the spinning axis, thus preventing the formation of a false twist between the clamping line of the front rollers of the drafting unit and the entrance to the spinning tip. Another function of the FFE is to help deflect the trailing ends of the fibres away from the fibre ribbon, which can then be twisted by nozzle air (Schaeffler 2007).

Several methods of determining the ratio of wrapper fibres to core fibres (or the percentage of wrapper fibres) in air-jet spun yarn have been published.

Soe et al. (2004) untwisted Vortex spun yarn of count 20 tex made of cotton fibres using a hand twister until reaching zero twists of wrapped fibres. They separated thin layers of untwisted fibres, took a digitised longitudinal view and counted the untwisted wrapper fibres. They have found that the wrapper fibres constituted 32 % of the total fibre content, and 11% of the core fibres were transformed into wrapper fibres. The method is demanding,

the fibres are not evenly distributed in the yarn structure and around the core. Some fibre ends tend to be tightly embedded in the yarn core, making it very difficult to separate or count them accurately. We can assume that some fibres may be counted more than once in this method.

Tyagi et al. (2004a), using the tracer-fibre techniques, reported that PES or cotton Vortex spun yarns contain 40 % – 50 % wrapper and wild fibres. The disadvantages of this method are that the traced fibres form only a small proportion of the fibres and do not include all the wrapping fibres. The longitudinal images show only the surface of the yarn, and the number of wrapping fibres below the edge wrapping fibres cannot be determined. The relative simplicity of the method is an advantage.

Erdumlu et al. (2012) calculated the ratio of wrapper and core fibres in carded cotton vortex spun yarns based on the weight of wrapper fibres and core fibres in short yarn sections. They presented the ratio as 0.43 - 0.9 based on yarn count. The method is not described in much detail, and the length of the section to be untwisted is not specified. The disadvantages are the great precision and labour required in separating the core and wrapping fibres, and the great accuracy in weighing.

Shang et al. (2016) used the longitudinal views of yarn taken with a scanning electron microscope to measure the wrapping angle, appearance diameter of the yarn, and helix pitch of the wrapper fibre layer and visually observed the number of wrapper fibres of the 100 % viscose Vortex yarns produced with various spinning pressures. Although the authors did not count the wrapper fibres, they conclude that as the nozzle pressure increases, the number of wrapped fibres and the yarn tenacity rise while the wrapping angle changes only slightly.

Leitner and Schwippl (2015) claim that the percentage of wrapper fibres can be in the range of 15 % - 30 % of the total number of fibres, depending on yarn count. They have analysed Rieter air-jet spun yarns made of Lyocell fibres, but they did not describe the method used.

Eldeeb et al. (2016) determined the percentage of wrapping fibres by comparing the volume of the wrapping fibre ribbon to the total yarn volume using microscopic images of longitudinal views of 100 % Viscose and 100 % Lyocell yarns produced on a Rieter air-jet spinning machine. They have found out that the yarns have 30% of wrapper fibres. This is a relatively subjective method of determining the percentage of wrapper fibres.

Mertová and Moučková (2020) identified wrapper and core fibres in 100% Viscose Rieter air-jet spun yarn from microscopic images of the yarn cross-section based on the size and deformation of fibre cross-sections. The authors used the frequency method (direct calculation) and reported that the ratio of wrapper fibres to all fibres in the yarn cross-section varies between 0.21 – 0.26. This method is time-saving. However, its disadvantage is the subjective determination of the boundary between the yarn core and the fibre cladding in the case of fibres with a non-circular cross-section. Therefore, this method is best suited for yarns with fibres of circular cross-section.

Vyšanská and Moučková (2025) proposed a method for measuring the percentage of wrapper fibres using computed tomography (CT) cross-sections through a yarn. They identified the wrapper and core fibres based on an evaluation of fibre inclination in two optimally spaced images of virtual yarn cross-sections using an image analysis tool - image arithmetic. They reported that the percentage of wrapper fibres in 100% Lyocell air-jet spun yarn is 36.3%. The advantage of this method is its simplicity; it does not destroy the yarn. The disadvantage is that only a very small section of yarn, approximately 3 mm, can be processed. To verify results, it is necessary to

process and measure a large number of sections, that is, CT images. This method requires specialised laboratory equipment; a computed tomography scanner must be available.

The principles of yarn production are similar across air-jet spinning machines, made by different textile machine manufacturers. However, these machines vary in construction, nozzle design, and parameters. For the Rieter air-jet spinning machine, the nozzle geometry and the fibre feeding element in front of the spinning tip in the nozzle housing differ from those of the MVS machine. These differences may lead to distinct trends in the relationships among machine process variables, yarn structure, and yarn properties, including the percentage of wrapper fibres in air-jet-spun yarn.

This paper introduces a novel method for identifying wrapper and core fibres in air-jet spun yarn using image analysis of yarn cross-sections, from which the percentage of wrapper fibres is subsequently calculated. Unlike the subjective approach proposed by Mertová and Moučková (2020), this method defines the boundary between the core and wrapping layers using objective, rule-based criteria. The new methodology is compared to other existing methods and is verified on a set of air-jet spun yarns produced with various spinning nozzle spacings (L). This spinning variable is expected to alter the structure of the air-jet spun yarn, which is examined in this study through the percentage of wrapper fibres and packing density. Because these structural parameters fundamentally affect yarn processing and mechanical performance, the subsequent part of this work examines the effect of the spinning nozzle spacing (L) of the air-jet spinning machine on selected yarn properties, including tenacity, breaking elongation, and hairiness. Consequently, this study extends existing knowledge regarding the relationships among the distance between the front roller nip line and the inlet of the spinning tip, the percentage of wrapper fibres, and the selected properties of air-jet spun yarn.

Material and methods

Lyocell yarns (100%) with linear densities of 20 and 30 tex were produced on a Rieter J20 air-jet spinning machine. To investigate the effect of the spinning nozzle spacing (L), three distinct yarn sets were manufactured using the following configurations: standard spacing (19.6 mm, with the spinning nozzle housing designated as Z-1), shorter than standard (17.6 mm, housing designated as Z-3), and longer than standard (21.6 mm, housing designated as Z+1). All other machine parameters were kept constant, except for the draft ratio, and are detailed in Table 1. The nominal fineness of the Lyocell fibres was 1.3 dtex, with a staple length of 38 mm.

Table 1 Air-jet spinning parameters

Yarn count	20 tex	30 tex
Sliver weight	3 620 tex	4 110 tex
Machine type	J20	J20
Total draft	181	137
Delivery speed	380 m.min^{-1}	380 m.min^{-1}
Spinning pressure	6.0 bar	6.0 bar

Spinning nozzle specifications (twist direction/amount of twist holes, diameter and angle)	Z / 4 x 0.60mm, 60°	Z / 4 x 0.60mm, 60°
Spinning tip type/ diameter / a-measurement	U/1.2 mm/0.8 mm	U/1.2 mm/0.8 mm
Spinning nozzle housing with fibre feeding element	Z-3 / Z-1 / Z+1	Z-3 / Z-1 / Z+1
Spinning nozzle spacing *L* [mm]	17.6 / 19.6 / 21.6	17.6 / 19.6 / 21.6
Spinning draft	1.00	1.00

The selected macroscopic longitudinal views of the produced yarns are shown in Fig. 4 a-f.

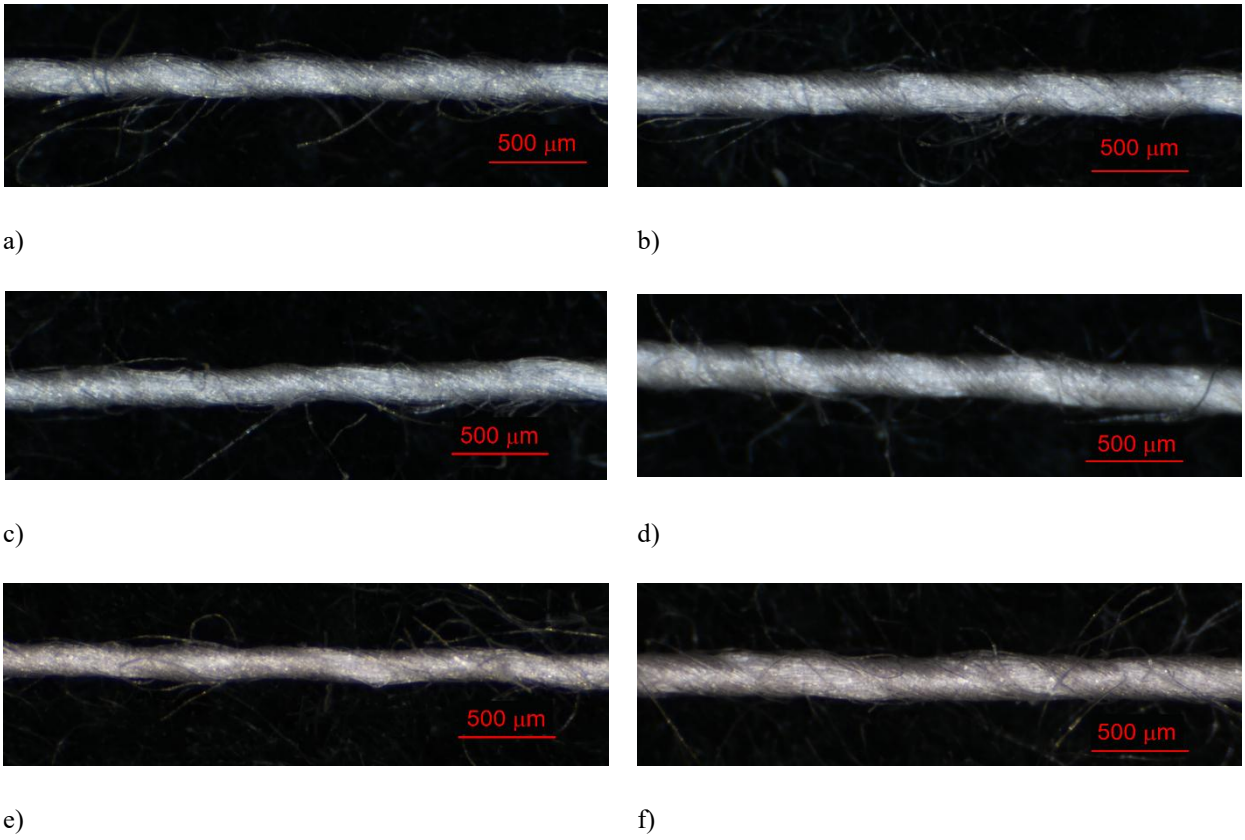


Fig. 4 Longitudinal view on produced yarns with different spinning nozzle spacing: Yarn count 20 tex, spinning nozzle housing Z-3 (a); Yarn count 30 tex, spinning nozzle housing Z-3 (b); Yarn count 20 tex, spinning nozzle housing Z-1 (c); Yarn count 30 tex, spinning nozzle housing Z-1 (d); Yarn count 20 tex, spinning nozzle housing Z+1 (e); Yarn count 30 tex, spinning nozzle housing Z+1 (f)

1.1 Determining the percentage of wrapper fibres

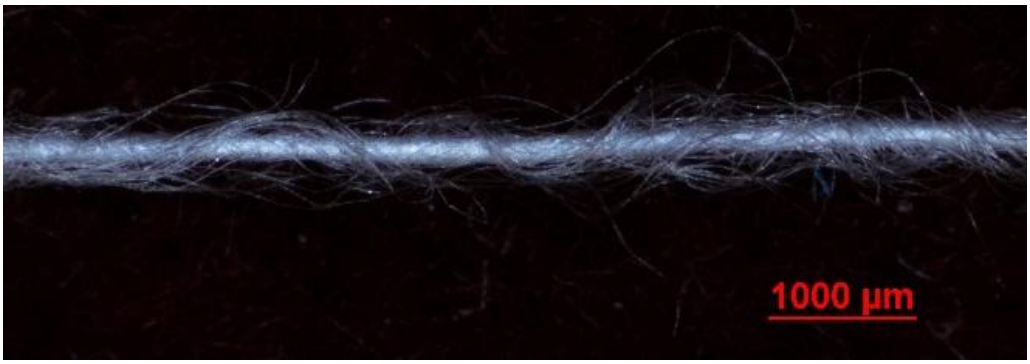
In this section, we evaluate selected methods for determining the wrapper fibers percentage and present a novel method for identifying wrapper and core fibres in air-jet spun yarn, enabling the subsequent calculation of the wrapper fibre percentage.

1.1.1 Weighting of wrapper fibres and core fibres in short yarn sections

Following the method described by Erdumlu et al. (2012), the yarn was manually untwisted under a microscope (Figs. 5a and 5b). As illustrated in Fig. 5b, it is impossible to distinguish between core and wrapper fibres after untwisting; the wrapper fibres form an entangled web that cannot be extracted from the structure because they remain anchored at one end within the yarn core. In a subsequent attempt, a 2 cm-long yarn section was cut (see Fig. 6a), and the wrapper fibres were manually separated. However, the wrapper fibres located at the core/wrap boundary were tightly held by the cohesive forces of the core fibres. Consequently, attempting to separate them caused the core fibres to untangle as well (Fig. 6b). Due to these practical limitations and the unfeasibility of the experimental yarns, this method was abandoned.

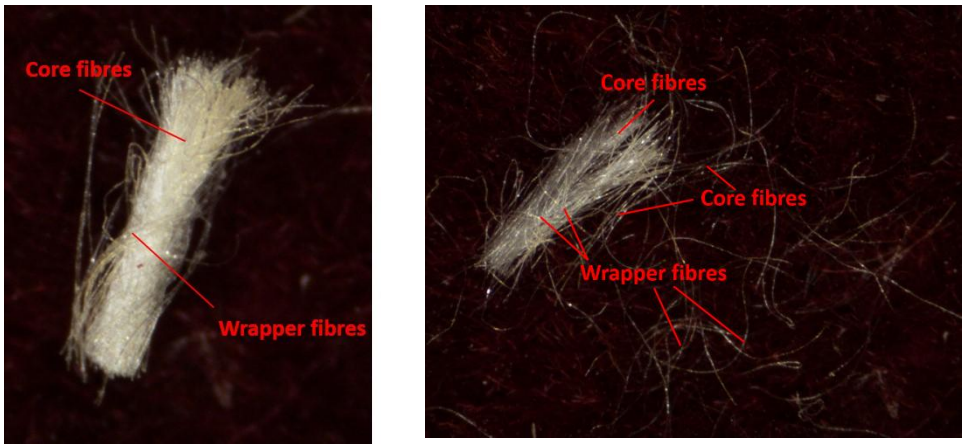


a)



b)

Fig. 5 Microscopic image of Rieter air-jet spun yarn 30 tex (spinning nozzle housing Z-1) before (a) and after (b) manual untwisting



a) b)

Fig. 6 Microscopic image of a cut section of air-jet spun yarn (a), separated fibres (b)

1.1.2 Methods using yarn cross sections

The methods used to determine the percentage of wrapper fibres presented in this publication are based on the analysis of yarn cross-sections prepared in accordance with Internal Standard No. 46-108-01/01 "Recommended procedure for preparation of samples: soft and hard sections (slices)". This standard explains the 'soft slices' method used for making yarn cross sections. According to this standard, each yarn sample was fixed in a medium made of a warm mixture of beeswax and paraffin. After hardening, 15-µm-thick slices were produced using a specialised technique with a microtome. A drop of xylene was applied to each slice to dissolve the wax and paraffin, and the cross sections were then examined under a downlight microscope at a resolution of 0.27 µm/pixel. From the individual images of the yarn cross sections, it is possible to measure the yarn packing density, yarn diameter, and the number of fibres. These parameters are described in Chapter 1.2.

The methods used to determine the wrapper fibre percentage presented in this study are based on the analysis of yarn cross-sections prepared in accordance with Internal Standard No. 46-108-01/01 ("Recommended procedure for preparation of samples: soft and hard sections (slices)"). This standard describes the 'soft slices' method employed for preparing yarn cross-sections. According to this procedure, each yarn sample was embedded in a warm mixture of beeswax and paraffin. After hardening, 15-µm-thick slices were cut using a microtome. A drop of xylene was then applied to each slice to dissolve the wax and paraffin matrix. The cross-sections were subsequently examined under a reflected-light microscope at a resolution of 0.27 µm/pixel. From the individual cross-sectional images, the yarn packing density, yarn diameter, and the number of fibres can be determined; these parameters are detailed in Section 1.2.

One of the established methods utilising yarn cross-sections is the frequency method (Mertová and Moučková, 2020).

Frequency method

The frequency method for determining the wrapper fibre percentage assumes that the yarn core consists of a bundle of approximately parallel fibres, reinforced by wrapper fibres that wrap helically around it. The model is shown in Fig. 7.

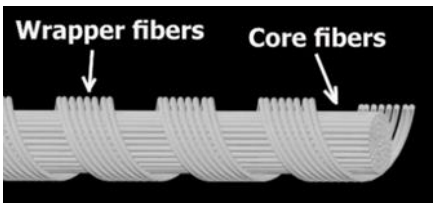


Fig. 7 Ideal structure of air-jet spun yarn (Eldeeb et al. 2016)

The image of the yarn cross-section captured in transmitted light, along with its geometric reconstruction, is shown in Fig. 8. Under the assumption that the air-jet spun yarn core consists of a bundle of parallel fibres aligned with the yarn axis, these core fibres exhibit a circular cross-section with a minimal area. In contrast, a wrapper fibre, which is oriented obliquely within the yarn structure (forming the surface ribbon), displays an elliptical cross-section in the transverse plane, resulting in a larger apparent area. Consequently, fibres with a cross-sectional area exceeding that of the parallel core fibres are classified as belonging to the wrapper layer (Fig. 8a).

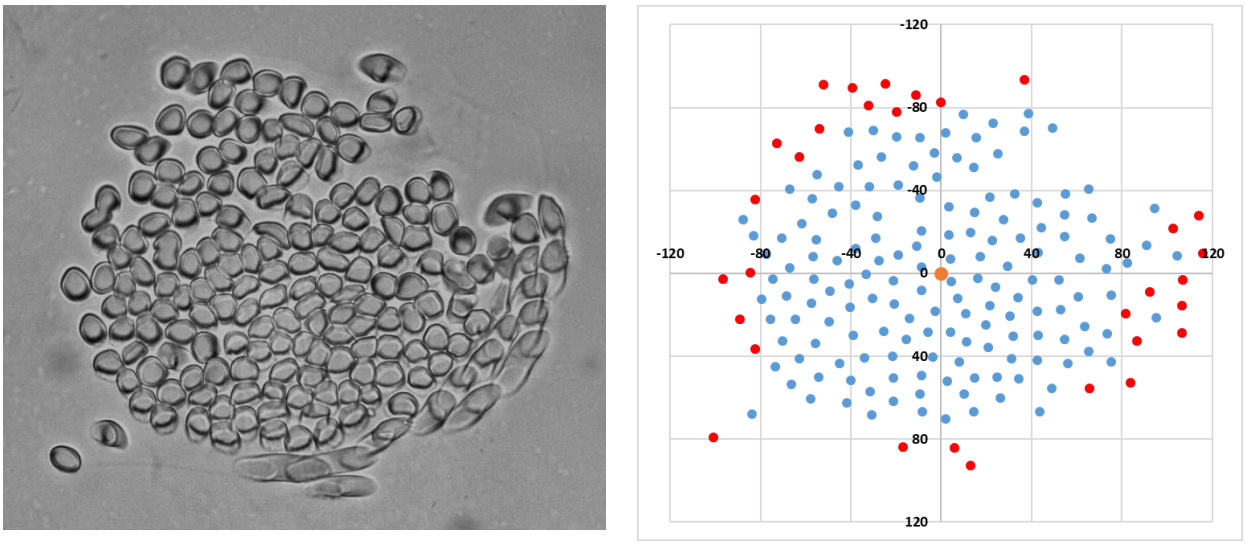
To generate the reconstruction of the yarn cross-section (Fig. 8b), the centres of individual fibres were marked based on their cross-sectional boundaries. Within this framework, the fibres in the ribbon and the core were initially selected separately and subjectively according to their visual appearance. The output of this procedure is a dataset containing the spatial coordinates of individual fibres, along with the total number of fibres in both the core and the ribbon. Subsequently, the percentage of wrapper fibres was determined from the relative frequencies of the wrapper and core fibres. The relative frequency of the number of wrapper fibres (ν_{wf}) in the yarn cross-section was calculated using Equation (1):

$$\nu_{\mathrm{wf}} = \frac{n_{\mathrm{wf}}}{n_{total}}, \tag{1}$$

where n_{wf} is the average number of wrapper fibres, and n_{total} is the total number of fibres in the yarn cross-section.

Nine images from each yarn were analysed.

Fig. 8b and Fig.11 show an example of the reconstruction of fibre centres in the yarn of count 30 tex spun using the Z-3 spinning nozzle housing. The fibre centres are marked in orange, the wrapper fibres are red, and the fibres within the yarn core are blue.



a) b)

Fig. 8 Cross-section of air-jet spun yarn – spinning nozzle housing Z-3, yarn count 30 tex, real microscopic image (a), reconstruction of the yarn cross-section - centre of the yarn (orange point) and centres of individual fibres (b)

Direct method and modification of the direct method

The weakness of the frequency method is the subjective matching of fibres to the core or ribbon. The new suggested method, so called direct method, follows on from the frequency method and eliminates this problem by classifying fibres into two groups, core or ribbon, based on specified rules, not subjectively. It also involves processing yarn cross-sections differently than the earlier method.

In the first step a cross-section of a single bundle of parallel fibres taken from the slivers, was created and processed, see Fig. 9. Cross-sections of the fibre bundle were created in the same way as the yarn cross-sections. The procedure is described above in chapter 1.1.3. The areas of the fibres were measured using image analysis from the binary image of the fibre bundle. The goal was to obtain information about the variability of the fibre area in a cross-section of a parallel fibre bundle. We measured that the fibre area in the cross-section of the fibre bundle has a mean value of 111 μm², with a confidence interval of [110;112] μm².

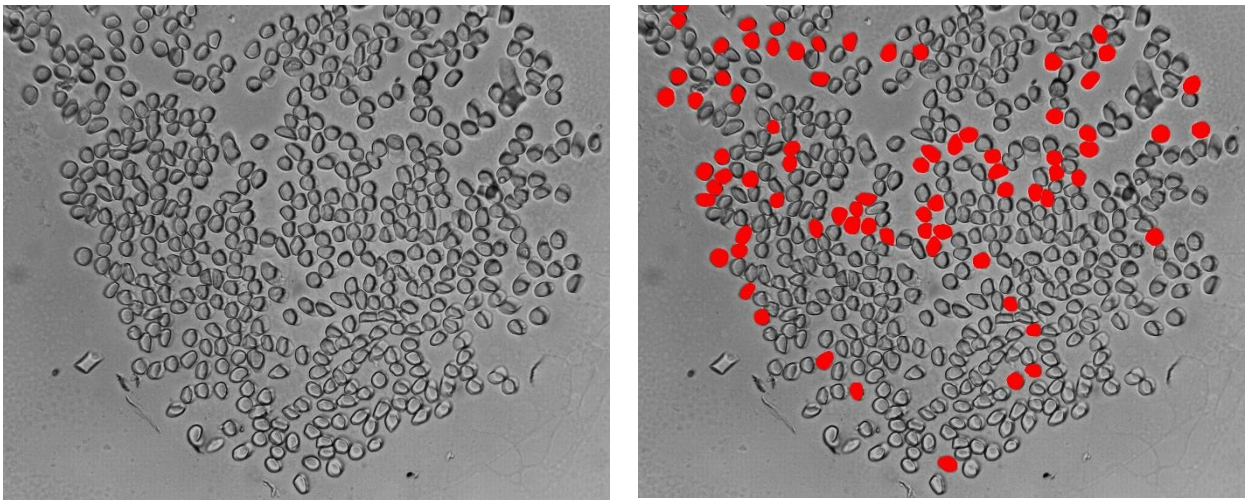
The second step was to generate a binary image of the air-jet yarn, in which all fibre sections were identified and measured (see Fig. 10). The core/wrapping boundary was defined as the upper limit of the 95% confidence interval of the mean cross-sectional area of the fibre.

In the third step, fibres with an area greater than 112 μm² were classified as wrapper fibres. The percentage of wrapper fibres was then calculated using equation (1).

Because the method is time-consuming, only one image per yarn type was processed. The preparation of the yarn cut itself takes approximately five days. Processing the cut using image analysis cannot be done automatically; each fibre cross-section must be marked individually.

When analysing images evaluated using the direct method, it was found that fibres with a cross-sectional area greater than 112 μm² are also located near the centre of the yarn. Therefore, a modification of the original direct

method was proposed (Figs. 10a, b). This method's modification specifies that the wrapper fibres must be at a certain distance from the yarn axis.



a) b)

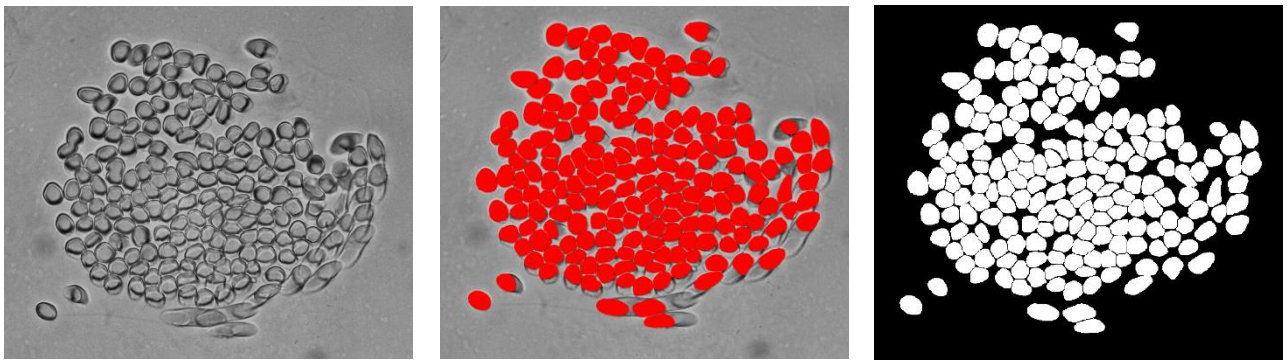
Fig. 9 Lyocell fibres parallel bundle, realistic image of a cross-section of a bundle of parallel fibres (a), illustration of basic fibre parameter measurements (b)

According to the modified direct method, fibres that meet two conditions belong to the wrapping layer (ribbons):
1) The cross-sectional area is greater than 112 microns.
2) Fibres lie on a radius larger than radius r. The r radius is determined based on knowledge of the parameter Z and the fibre inclination angle β, see equation (2):

$$r = \frac{\tan\beta}{2\pi Z}, \quad \cos\beta = \frac{s}{s^*}, \tag{2}$$

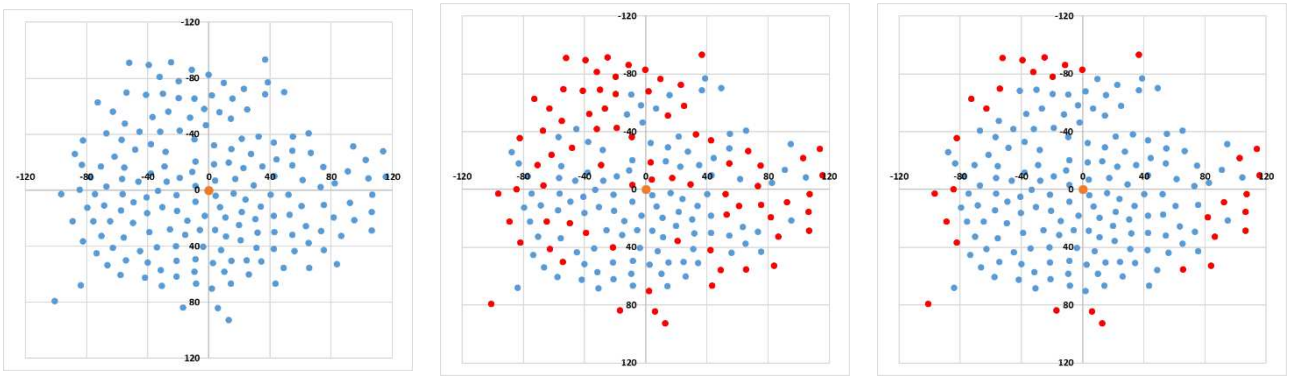
Where Z is the number of wrapper fibre coils per meter, s is the fibre cross-sectional area and s^* is the fibre sectional area.

The percentage of wrapper fibres is determined as the ratio of the number of wrapper fibres to the total number of fibres in the yarn cross-section according to formula (1). The difference is therefore only in the method of assigning fibres to the wrapper layer – ribbons.



a) b) c)

Fig. 10 Cross-section of air jet spun yarn - spinning nozzle housing Z-3, yarn count 30 tex, real image (a), overlay image (b), binary image (c)



a) b) c)

Fig. 11 Cross-section of air jet spun yarn, spinning nozzle housing Z-3, yarn count 30 tex, reconstruction of the cross-section - centre of the yarn and individual fibres (a), Direct method (b), Direct method – modification (c)

1.2. Yarn packing density

The measure of fibre compactness is expressed by the ratio between the volume occupied by the fibres and the total volume of the fibre assembly in the three-dimensional space. Neckář and Das (2012) define the variable μ as yarn packing density:

$$\mu = \frac{V}{V_c}, \quad \mu \in \langle 0, 1 \rangle \tag{3}$$

We measured the yarn packing density, yarn diameter, and the number of fibres according to the internal standard 22-103-01/01 “Yarn packing density. Direct method and Secant method” from individual images of the yarn cross sections. Based on this standard, we used the secant method to determine the packing density as a function of yarn radius. The secant method is suitable for yarns made of short-staple fibre or other highly twisted yarns, where it is difficult to recognize the individual contours of fibre sections. Additionally, because there are over 200 fibres in the experimental yarns of count 30 tex, using the secant method is more suitable. The main idea of the secant

method is to first locate the centre of gravity of the individual fibres in the yarn cross-section and then reconstruct their cross-sectional areas considering fineness, density, fibre position, and yarn twist. A detailed description of the method used to determine the fibre packing density in the yarn cross-section is available in Neckář et al. (1988). Here, we use the wrapper-fibre ribbon helix pitch h to calculate the wrapped-fibre ribbon twist Z (Mertová and Moučková 2020) as follows:

$$Z = \frac{1}{h}. \tag{4}$$

The effective yarn diameter d_{eff} was estimated by interpolating the measured packing density μ and corresponds to a radial packing density level of 0.15 (Neckář and Das 2019). The effective packing density μ_{eff} is the ratio of the effective fibre area S_{eff} to the effective area of the circle Sc_{eff}, which is given by the effective diameter d_{eff}.

$$\mu_{\text{eff}} = S_{\text{eff}} / Sc_{\text{eff}} \ . \tag{5}$$

1.3. Effect of spinning nozzle spacing on air-jet spun yarn properties

Changes in the air-jet spinning machine parameters affect the structure of the air-jet spun yarn. The change in structure subsequently affects the properties of the air-jet spun yarn, particularly its tensile properties, hairiness and yarn diameter. One of the air-jet spinning machine parameters is the spinning nozzle spacing (the distance between the front rollers of the drafting device and the spinning tip inlet). We assume that the spinning nozzle spacing will affect the ratio of core fibres to fibres in the wrapper layer, and that changes in yarn structure will consequently affect yarn properties. Therefore, we investigated the influence of the spinning nozzle spacing on yarn tenacity, yarn braking elongation, yarn hairiness and yarn diameter.

Tensile strength and elongation were measured in accordance with ISO 2062:2009 using an Instron 4411 testing machine. The following conditions were used: gauge length: 500 mm; crosshead speed: 500 mm/min. The yarns were tested with a pretension of 0.5 cN/tex. A total of 150 measurements were performed for each yarn variant; the results were statistically analysed, and the graphical results are shown in Fig. 15.

Hairiness was measured using a Zweigle Hairiness Tester G 567. Measurement conditions: yarn feed rate 50 m/min. Length of the measured yarn section per measurement: 100 m. Hairiness was evaluated using the summary criteria *S12* and *S3*. Summary criterion *S3* indicates the total number of protruding fibres in the length categories 3–15 mm from the yarn body. Summary criterion *S12* indicates the total number of protruding fibres from the yarn body in the length categories 1 and 2 mm. A total of 10 measurements were performed for each yarn variant.

Results and discussion

2.1. The percentage of wrapper fibres

The percentage of wrapper fibres was determined using three methods (frequency, direct, and modified direct) described in Chapter 1.1. The measurement results obtained with all methods are presented in Table 2.

Table 2 Wrapper fibres percentage

Yarn count		20 tex			30 tex		
The spinning nozzle housing		Z-3	Z-1	Z+1	Z-3	Z-1	Z+1
Spinning nozzle spacing *L* [mm]		17.6	19.6	21.6	17.6	19.6	21.6
Wrapper fibres percentage [%]	Frequency method	24	30	25	25	28	27
	Direct method	34	29	31	41	18	23
	Direct method (modification)	22	19	22	30	17	19

Fig. 12a and Fig. 12b illustrate a graphical representation of the percentages of wrapper fibres for the frequent method and the direct method, respectively, as a function of spinning nozzle spacing.

Table 2 and Figs. 12a, b show only the average values of the wrapper fibres percentage. To determine the representative variability of the results, it is necessary to process a larger number of sections using the direct method. Only the applicability and principle of the method are presented here.

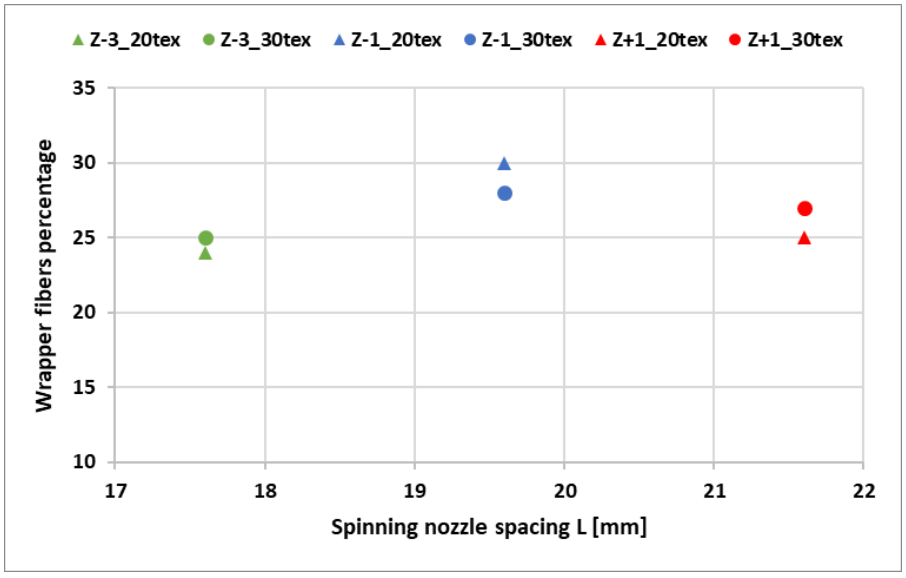


Fig. 12a Influence of the spinning nozzle spacing *L* on wrapper fibres percentage – Frequent method

In the case of the frequent method, the highest percentage of wrapper fibre applies to both yarn count levels for yarns with a medium spinning nozzle spacing *L* (spinning nozzle housing Z-1).

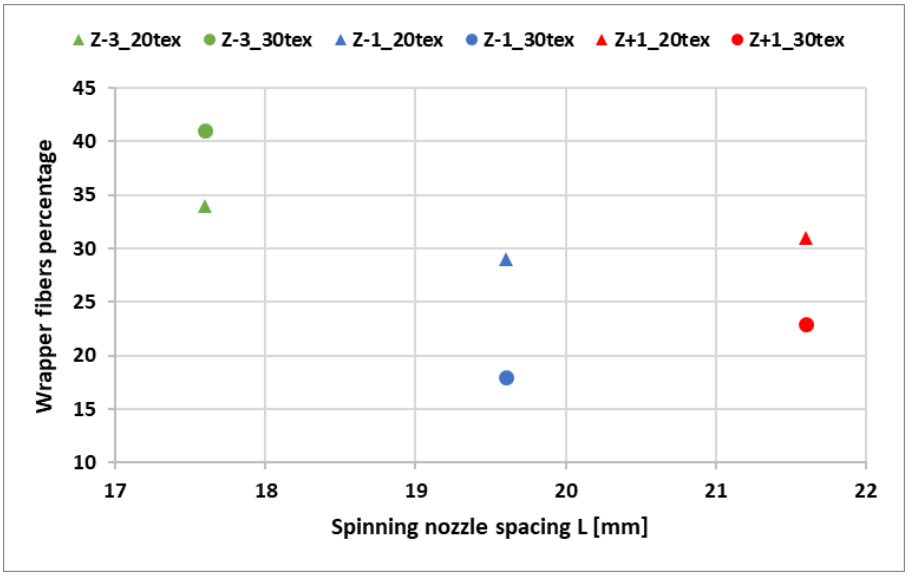


Fig. 12b Influence of spinning nozzle spacing *L* on wrapper fibres percentage – Direct method

The highest number of wrapper fibres determined using the direct method was found in yarns spun with the shortest spinning nozzle spacing *L*.

Both methods are based on processing the same microscopic images of yarns, so the difference can only be explained by the processing method. While the frequency method relies on subjective differentiation between core and wrapper fibres, the direct method distinguishes between these two fibre categories according to precisely defined rules. The trend given by the direct method is logically explainable and corresponds to the structural and mechanical properties of air-jet spun yarns.

The highest number of wrapper fibres determined using the direct method is found in yarns spun with the shortest spinning nozzle spacing (and thus the shortest FFE) in the spinning nozzle housing Z-3. This could be because the spinning nozzle spacing of the spinning nozzle housing Z-1 and Z+1 is too long. If these spacing, respectively, elements are too long, the leading ends of the fibres do not have to be fixed in the centre of the yarn as required. Loose fibre ends can be pulled out of the fibre bundle by the air flow and become waste.

Results obtained using the direct modified method follow the same trend as those obtained using the direct method. However, due to the second condition - distance from the centre of the yarn, the wrapper fibre percentage is lower (see table 2).

The results of all compared methods show that the percentage of wrapper fibres in the yarn is influenced by fineness and spinning nozzle spacing settings. Previous studies, such as Erdumlu et al. (2012) and Leitner and Schwippl (2015) have confirmed the effect of yarn fineness on the percentage of wrapper fibres. The relationship between yarn fineness and wrapper fibre percentage is also influenced by the experimental method used to determine the percentage of wrapper fibres. The divergence in trends between the two methods is shown in Fig. 12a and 12b.

The values of the wrapper fibre percentage are comparable to those reported by other authors. They most often range around 30%, which is also confirmed by our results. In addition to the influence of fineness and spinning

nozzle spacing, the percentage of wrapping fibres is also influenced by the raw fibre material, fibre fineness, fibre bending rigidity and cross-sectional shape, and friction coefficient, which affect fibre migration in general.

Comparison of methodologies

Among the methods listed above, the frequency method is the least time-consuming. This allows processing a larger number of images, leading to lower data variability. The disadvantage is the obvious subjectivity involved in identifying the wrapper fibres. In the case of subjective evaluation, it is also necessary to understand the relationship between the material, the spinning unit configurations on the air-jet spinning machine, and the structure and properties of the air-jet spun yarns. The laboratory technician must have some experience in determining when a fibre is a core (parallel) fibre and when it is a wrapper (inclined relative to the yarn axis) fibre. Even so, the evaluation and processing of yarn images remain highly subjective.

The direct method is more time-consuming than the frequency method. If images of yarn cross-sections of sufficient quality are unavailable, it is not possible to obtain a binary image automatically. Each fibre must be traced by hand. Images of sufficient quality must be prepared to identify the edges of the upper cross-sectional surface of the fibres. The difference between the surface of a fibre parallel to the yarn axis and that of an inclined fibre is small, so precision is required when tracing. The experiment showed that some fibres near the centre of the yarn have a cross-sectional area greater than the core/cover boundary. This is due to imperfect parallelism of the fibres with the yarn axis, the fibre bundle, or the method used to create the cross-sections. The observed cross-sectional area of the fibres is sensitive to the angle of inclination of the fibres in the yarn. The cross-sectional area of some fibres near the centre of the yarn may be larger. Based on this finding, a modified method was proposed. The modification involves specifying a certain distance between the wrapper fibre and the centre of the yarn. This distance is determined by the yarn twist (in the case of air-jet spun yarn, wrapper fibre ribbon twist) and the corresponding fibre cross-sectional area in the yarn section.

Although the modified direct method utilizes the same image processing workflow and shares the disadvantage of high time consumption and strict binary image precision, it offers a major advantage: fibres situated in the immediate yarn centre are correctly excluded from the wrapper count.

In general, methods that determine fibre parameters from yarn cross-sections are time-consuming and, of course, require expensive laboratory equipment.

In terms of the demands of laboratory technique. The measurement of fibre parameters inside the yarn using image analysis requires special equipment, such as a microscope, microtome, special software (image analysis, for example, NIS-Elements AR 2.30), etc. and is usually found in research centres, not in common laboratories.

Unfortunately, alternative macro-level approaches, such as weighing or longitudinal yarn inspection, lack the necessary accuracy and reliability.

An innovative alternative, though not entirely free from subjective interpretation, involves the analysis of 3D yarn volumes via computed tomography (CT), as reported by Vysanska and Mouckova (2025). This non-destructive method was applied to a 100% Tencel air-jet spun yarn of 23 tex produced with a Z-1 nozzle housing, yielding a

wrapper fibre percentage of 36.3%. This value is highly comparable to the results achieved with our proposed direct method. The CT-based approach shares a similar underlying logic with the direct method by utilizing fibre spatial position and inclination; however, it processes the fibres in a three-dimensional space rather than a single transverse plane.

Soe et al. (2004) studied the structure of spun yarns with the fibre tracing method. Their results indicated that, because of twisting and fibre migration, some fibres are classified as both core and wrapper fibres - one end belonging to the yarn core and the other to the wrapping layer. To verify this, it is essential to analyse multiple cross-sections along a longer yarn segment.

It must be noted that all methods reviewed herein measure the wrapper fibre percentage over relatively short yarn lengths. Air jet-spun yarns generally have a lower mass irregularity value compared to other types of yarn. Nevertheless, due to fluctuations in mass, it is necessary to measure the percentage of wrapper fibres over a length greater than a few centimetres.

2.2. Packing density

Table 3 displays the effective packing density and diameters of all experimental yarns. An example of packing density as a function of yarn radius is shown in Fig. 13a. Fig. 13b illustrates the effect of spinning nozzle spacing L on the radial packing density curve for yarn of count 30 tex. The graph indicates that the radial packing density functions and effective packing density are nearly identical. The same trend has been observed for radial packing density with yarns of count 20 tex.

Table 3 Effective packing density and effective diameter of the experimental yarns

Yarn count	20 tex			30 tex		
The spinning nozzle housing	Z-3	Z-1	Z+1	Z-3	Z-1	Z+1
The spinning nozzle spacing L [mm]	17.6	19.6	21.6	17.6	19.6	21.6
Packing density[-]/*CI	0.58/ *0.04	0.44/ 0.09	0.55/ 0.03	0.51/ 0.04	0.52/ 0.05	0.52/ 0.04
Yarn diameter [mm]	0.162/ 0.009	0.186/ 0.005	0.176/ 0.012	0.210/ 0.014	0.209/ 0.030	0.227/ 0.003

*) "CI" Margin of error (on the Significance level of 0.05%).

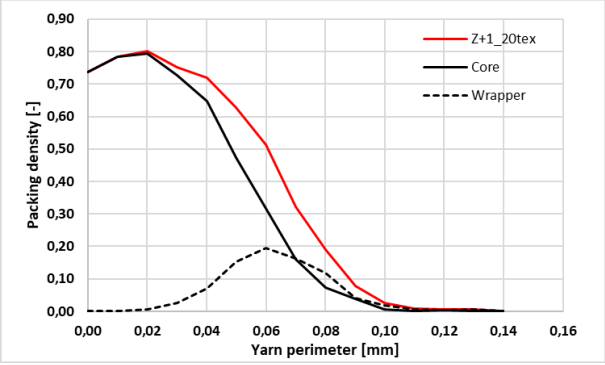


Fig 13a Radial yarn packing density as a function of yarn radius

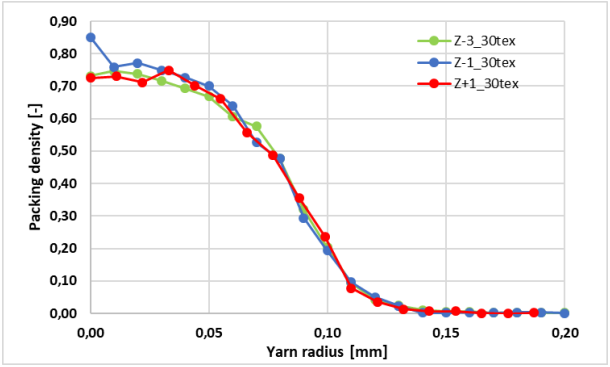


Fig 13b Radial yarn packing density as a function of yarn radius for several values of spinning nozzle spacing

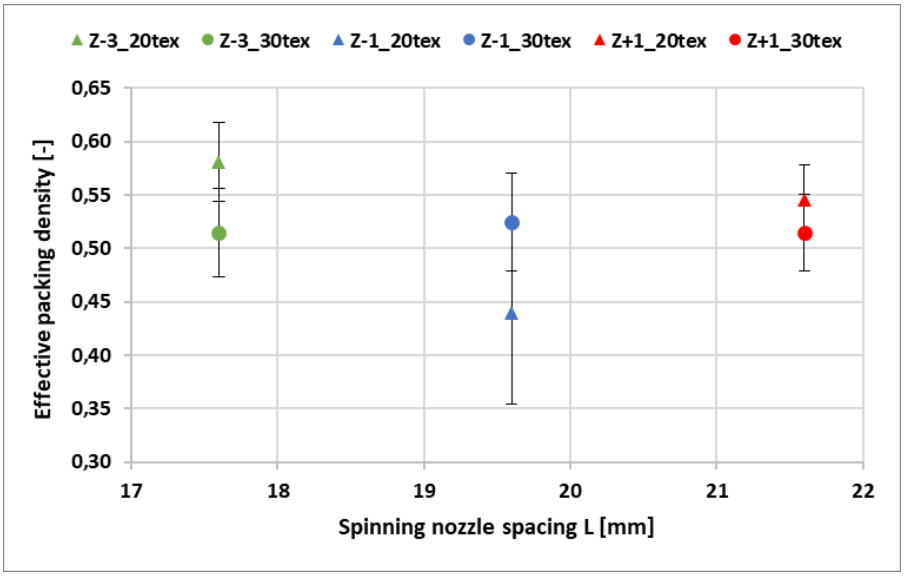


Fig. 14 Effective packing density as a function of the spinning nozzle spacing *L*

The effect of the spinning nozzle spacing *L* on the effective packing density value is shown in Fig. 14.

The average packing density value of yarn of count 20 tex, spun using the spinning nozzle housing Z-1 (Z-1_20tex), e.g. spinning nozzle spacing *L* = 19.6 mm is lower than the packing density values of the yarn spun with other spinning nozzle spacing *L*. However, due to the high data variability, the difference among all three values is statistically insignificant. Based on these results, we can conclude that the *L* setting has no effect on the packing density of yarns with a count of 30 tex and 20 tex. Yarn packing density is a parameter influenced by many factors. It depends not only on the yarn production technology and twist but also on the fineness and material. Yarns with a higher count (in tex unit) generally have a lower packing density value. This fact has been supported by numerous experiments and theories, e.g. Neckář and Das (2018). In this work, it was not be confirmed for yarns spun with the standard spinning nozzle spacing *L*, i.e. spinning nozzle housing Z-1.
From a statistical point of view, however, the used distance *L* has no statistically significant effect on the packing density value.

2.3. Effect of spinning nozzle spacing on air-jet spun yarn properties

The final results of the measurements of yarn tenacity, breaking elongation, and hairiness are presented in Table 4 and Fig. 15 and Fig. 16.

The tenacity and breaking elongation of the experimental yarns at both counts increased with increasing spinning nozzle spacing *L* (Fig. 15a, Fig. 15b). The yarns of count 30 tex showed lower tenacity and breaking elongation compared to yarns of count 20 tex. ANOVA analysis confirmed that these changes in tenacity and elongation were statistically significant (see Table 5). Additionally, the results highlighted the significant effect of yarn count and the interaction between distance *L* and yarn count.

Table 4 Selected properties of experimental yarns

Yarn count	20 tex			30 tex		
The spinning nozzle housing	Z-3	Z-1	Z+1	Z-3	Z-1	Z+1
The spinning nozzle spacing *L* [mm]	17.6	19.6	21.6	17.6	19.6	21.6
Tenacity [cN/tex]/*CI	19.3/0.3	20.6/0.3	21.7/0.3	13.8/0.3	19.2/0.3	21.1/0.2
Breaking elongation [%]	5.6/0.1	6.2/0.1	6.8/0.1	4.0/0.1	5.8/0.1	6.6/0.1
Hairiness *S3* [1/100m]	2.9/*2.0	2.4/1.4	4.4/1.0	3.6/1.5	1.4/0.6	2.1/1.2
Hairiness *S12* [1/100m]	1657/129	1326/35	1324/299	1547/91	907/54	874/59

*) "CI" Margin of error (on the Significance level of 0.05%).

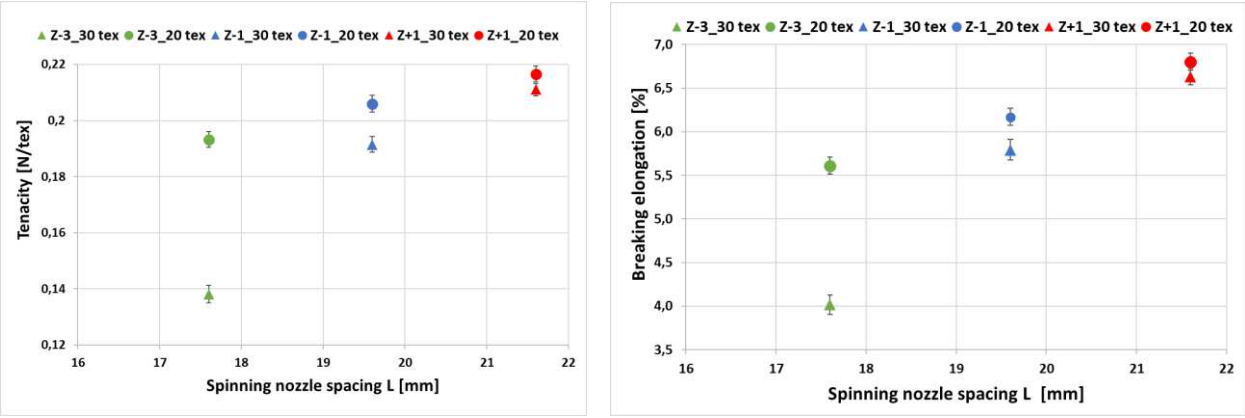
The tenacity and elongation of a yarn are usually affected by various factors such as the raw fibre material, the spinning technology employed, and the conditions during spinning. Additionally, the spinning technology influences the specific structure of the air-jet spun yarn.

The tensile strength and elongation of this yarn are significantly influenced by the wrapping ribbon of fibres, which wraps around the core fibres with a permanent twist. Important parameters of the wrapping ribbon include its height, the number of fibres, or more precisely the percentage of wrapping fibres that make it up, and the number of coils created.

The separation of the trailing ends of surface fibres (which then twist around the core and remain as wrapper fibres) during yarn formation occurs at the nip line of the front rollers of the drafting mechanism and at the inlet of the spinning tip (i.e., spinning nozzle spacing L), with the length of the fibre guide element FFE also having an influence.

For a longer distance L, it is necessary to use a spinning nozzle housing with a higher length of the fibre feeding element. A greater distance L and thus a longer FFE can improve core fibre straightening during its movement to the spinning nozzle tip, thereby enhancing the tenacity and elongation of the core fibre strand and, consequently, the final yarn.

To achieve the required tenacity, it is necessary not only to deflect a sufficient number of fibre ends but also to allow enough time for them to twist around the yarn core. Both factors are influenced by the spinning air pressure and the yarn delivery speed. For the yarn of count 30 tex, these two parameters were likely low, which is why this yarn exhibits lower tenacity the yarn of count 20 tex.

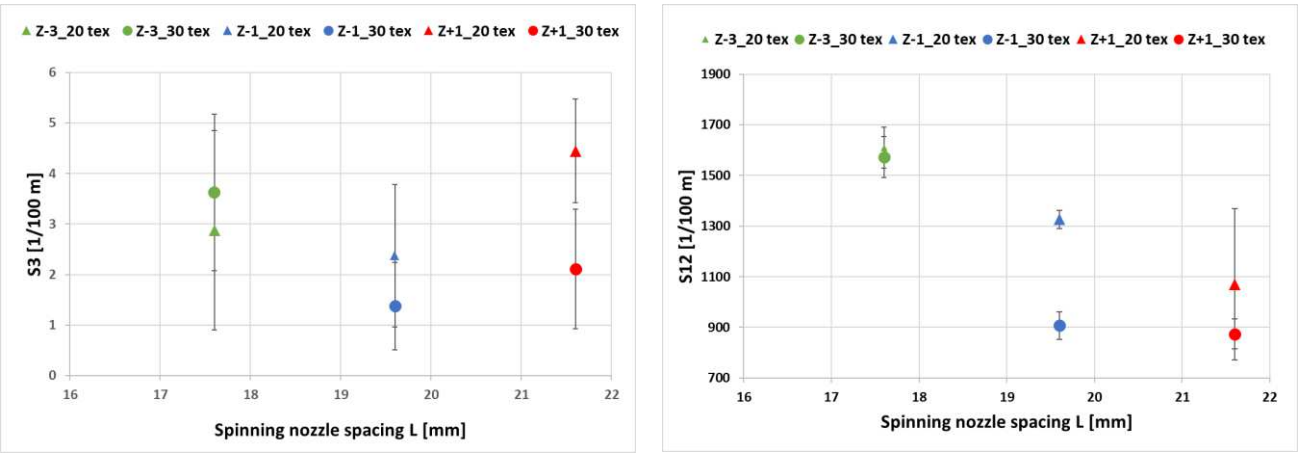


a) b)

Fig. 15 Influence of the spinning nozzle spacing *L* on the tenacity (a) and breaking elongation (b) of the air-jet spun yarns

The lowest yarn hairiness value *S12* was recorded for the yarn of count 30 tex produced with the longest spinning nozzle spacing (*L* = 21.6 mm); similarly, the yarn of count 20 tex exhibited the lowest hairiness value when the longest spinning nozzle spacing was used. Yarns produced with the shortest spinning nozzle spacing, on the other hand, achieved the highest hairiness values. This trend could be due to the fact that using a shorter spinning nozzle spacing (and thus a shorter FFE) results in less control over fibre control and thus higher hairiness. The results of the two-way ANOVA confirmed a significant effect of distance *L*, yarn fineness, and their interaction on the yarn hairiness *S12*.

For *S3* hairiness, a significant interaction between yarn fineness and spinning nozzle spacing was confirmed. However, the effects of the individual factors were not significant. The lowest hairiness values were achieved with yarns produced using a medium spinning nozzle spacing.



a) b)

Fig. 16 Influence of the spinning nozzle spacing *L* on the hairiness *S3* (a) and hairiness *S12* (b) of the air-jet spun yarns

Table 5 ANOVA Results

Factor	*S12*		*S3*		Tenacity		Breaking elongation	
	p-value		p-value		p-value		p-value	
L	3.39E-09	S*	0.589298	N*	0	S	0	S
Yarn Count	5.61E-05	S	0.700464	N	0	S	1.99E-53	S
Interaction	0.000528	S	0.004681	S	1.88E-62	S	9.32E-42	S

*) S – significant, N - no significant

2.3 The relationship between air-jet spun yarn structure and its selected properties

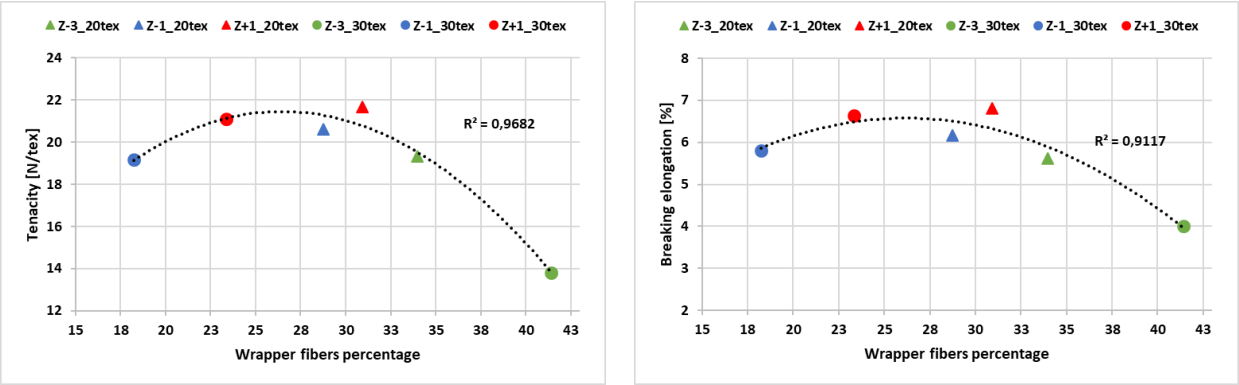
The influence of the air-jet spun yarn structure on its properties is discussed in terms of the wrapper fibre percentage. The relationship between the wrapper fibre percentage and the yarn's tenacity is shown in Fig. 17a. This relationship is not linear. The results show that as the wrapper fibre percentage increases, the yarn's tenacity increases. After exceeding a certain value of the wrapper fibre percentage, the strength decreases.

According to the assumptions, the structure of air-jet spun yarn consists of two parts: a core formed by parallel fibres and a wrapping layer - a ribbon - that takes a helical shape due to twisting. The mechanism of tensile force transmission differs in both parts. In the wrapper fibres, tensile force is distributed, so the fibres do not transmit tensile force perfectly. We assume that the core, consisting of a more or less parallel bundle of fibres, transmits tensile force more effectively. Inter-fibre friction in both parts also plays a role, and it is likely higher in the core due to twisting of the fibre ribbon.

It appears that once a certain threshold for the percentage of wrapper fibres is exceeded, the distribution of tensile force within the yarn becomes so significant that it exceeds the transfer of tensile and frictional forces between the fibres in the core. The question is: what is this critical percentage of wrapper fibres? For the set of experimental yarns, it is around 26 %.

A similar trend can also be observed between tensile strength and the percentage of packaging fibres; see Fig. 17b.

There is a significant correlation between hairiness and the percentage of cover fibres. This linear relationship is shown in the graph in Fig. 18. A higher percentage of cover fibres means more fibre ends are separated into the cover layer. Under the same spinning conditions (spinning air pressure, delivery speed), more of these fibres will remain untwisted, and thus yarns with a higher percentage of wrapper fibres may exhibit higher hairiness. This assumption is confirmed by the relationship shown in Fig. 18.



a) b)

Fig. 17 Influence of wrapper fibres percentage on yarn tenacity (a) and yarn breaking elongation (b)

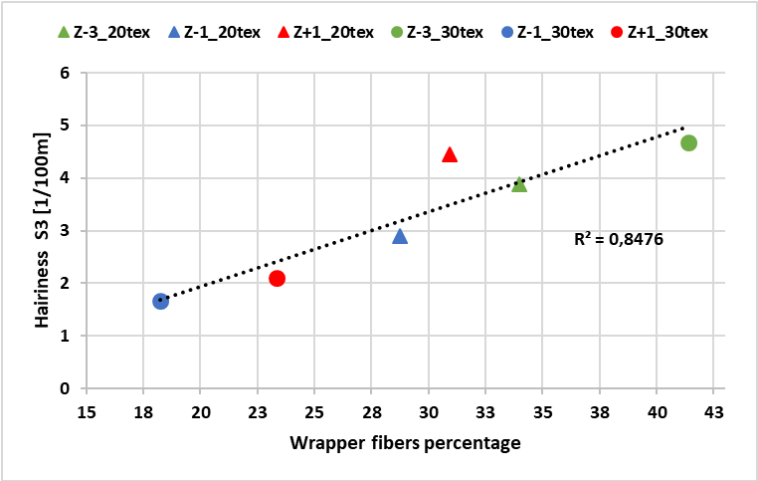


Fig. 18 Influence of wrapper fibres percentage on yarn hairiness *S3*

Conclusion

This study focused on developing a new methodology for determining a key structural parameter of air-jet spun yarn (the percentage of wrapper fibres) and optimising it. The methodology was tested on a set of air-jet spun yarns made from Lyocell fibres. At the same time, the influence of the air-jet spinning machine settings (specifically, spinning nozzle spacing) on the resulting yarn properties was analysed. Based on the results obtained, the following conclusions can be formulated:

A new “direct method” (and a modified version thereof) has been developed and validated to determine the proportion of wrapper fibres from yarn cross-section analysis. This method eliminates the subjectivity of the previously used “frequency method” by classifying fibres as core and wrapper based on precise geometric rules and analysis of centres of gravity in the cross-section. Although the method is more time-consuming, it provides the high accuracy necessary for detailed structural analysis.

The results confirmed that the spinning nozzle spacing (L) influences the formation of the wrapping ribbon and, consequently, its structural parameters and the yarn's technological properties.

Statistical analysis confirmed that L does not significantly affect yarn packing density but substantially affects tenacity, breaking elongation, and hairiness. Specifically, increasing the distance L (using longer fibre feeding elements) consistently improved yarn tenacity and elongation across both 20 tex and 30 tex counts.

Research has shown that the number of short protruding fibres ($S12$) decreased as the spinning nozzle spacing L increased, likely due to better fibre control resulting from a longer fibre feeding element.

A nonlinear relationship was observed between the ratio of wrapper fibres and yarn tenacity. Both tenacity and breaking elongation increase with the ratio of wrapper fibres only up to a critical limit (approximately 26% in our data set); beyond this limit, mechanical properties decline due to the distribution of tensile forces within the wrapping. For both tested counts (20 and 30 tex), increasing the spinning nozzle spacing led to significant improvements in tenacity and breaking elongation.

The established correlation between yarn hairiness and the wrapper fibre percentage suggests that a higher percentage of wrapper fibres increases the chances of Lyocell fibre ends protruding from the yarn body when the key spinning variables (spinning air pressure and delivery speed) are held constant.

This study thus extends our understanding of the relationships among the settings of an air-jet spinning machine, yarn structure, and yarn characteristics, enabling more accurate prediction and optimisation of the quality of air-jet spun yarns made from Lyocell fibres. The direct method presented here provides a robust and objective approach for future structural analyses of high-performance yarns.

Reference

Abdennadher A, Vincent M, Budtova T (2016) Rheological properties of molten flax- and tencel®-polypropylene composites: influence of fibre morphology and concentration. Journal of Rheology 60(1):191-201. https://doi.org/10.1122/1.4938224.

Basal G, Oxenham W (2006) Effects of some process parameters on the structure and properties of vortex spun yarn. Textile Research Journal 76(6):492-499. https://doi.org/10.1177/0040517506064253.

Basal G, Oxenham W (2001) Vortex Spun Yarn vs. Air-Jet Spun Yarn AUTEX Research Journal 3(3):96–101.

Basu A (2001) Progress in Air-jet Spinning. Textile Progress 29(3). Textile Institute Manchester p. 1. 1999.

Bhatti MRA, Tausif M, Mir MA, Umar M, Cassidy T (2019) Effect of key process variables on mechanical properties of blended vortex spun yarns. The Journal of The Textile Institute 110(6):932–940. https://doi.org/10.1080/00405000.2018.1532784.

Eldeeb M, Moučková E, Ursíny P (2016) Theoretical Analyses of Air Jet Yarn Strength. In: STRUTEX: Structure and Structural Mechanics of Textile Fabrics. Liberec: Faculty of Textile Engineering - Technical University of Liberec 2016 pp. 131-136. ISBN 978-80-7494-269-3.

Eldeeb M, Demir A (2018) Optimising the production process of Rieter air jet spun yarns and a model for prediction of their strength. Fibres and Textiles in Eastern Europe 26(1): 36–41. https://doi.org/10.5604/01.3001.0010.7794.

Eldeeb M and Mouckova E (2017) Numerical simulation of the yarn formation process in Rieter air-jet spinning. The Journal of The Textile Institute 108(7):1219–1226. https://doi.org/10.1080/00405000.2016.1230000.

Erdumlu N, Ozipek B (2010) Effect of the draft ratio on the properties of vortex spun yarn. Fibres & Textiles in Eastern Europe 18(3):38–42.

Erdumlu N, Ozipek B, Oxenham W (2012b) The structure and properties of carded cotton vortex yarns. Textile Research Journal 82(7):708–718. https://doi.org/10.1177/0040517511433150

Erdumlu N, Ozipek B, Oztuna AS, Cetinkaya S (2009) Investigation of vortex spun yarn properties in comparison with conventional ring and open-end rotor spun yarns. Textile Research Journal 79(7):585-595.

Ghosh A, Ishtiaque S, Rengasamy R (2005) Analysis of spun yarn failure. part i: tensile failure of yarns as a function of structure and testing parameters. Textile Research Journal 75(10):731-740. https://doi.org/10.1177/0040517505053956.

Guo H, Chen Z, Yu C (2008) Numerical study of an air-jet spinning nozzle with a slotting-tube. Journal of Physics Conference Series 96 012110. https://doi.org/10.1088/1742-6596/96/1/012110.

Guo Y, Tao X (2016) Fibre packing density in the cross-section of low torque ring spun yarn. Textile Research Journal 88(2):191-202. https://doi.org/10.1177/0040517516677225.

Internal standard No. 46-108-01/01 (2012) Recommended procedure for preparation of samples. Soft and hard sections. Liberec: Research Centre of Textile. Technical University of Liberec.

Internal standard No. 22-103-01/01 (2004) Yarn packing density. Secant method. Liberec: Research Centre of Textile, Technical University of Liberec.

ISO 2062:2009. Textiles — Yarns from packages — Determination of single-end breaking force and elongation at break using constant rate of extension (CRE) tester. 3rd ed. Geneva: International Organization for Standardization.

Karakan G (2019) Effect of pin spacer apparatus on the properties of knitted fabrics from cotton-tencel yarns. Industria Textila 70(02):125-132. https://doi.org/10.35530/it.070.02.1607.

Kılıc M, Okur A (2010) The properties of cotton-tencel and cotton-promodal blended yarns spun in different spinning systems. Textile Research Journal 81(2):156-172. https://doi.org/10.1177/0040517510377828.

Kim H (2023) Eco-friendly fibres embedded yarn structure in high-performance fabrics to improve moisture absorption and drying properties. Polymers 15(3):581. https://doi.org/10.3390/polym15030581.

Kuthalam S, Senthilkumar P (2013) Effect of fibre fineness and spinning speed on polyester vortex spun yarn properties. Fibres & Textiles in Eastern Europe 21(5):35–39.

Kuthalam S, Senthikumar P (2014) Influence of spindle air pressure and its direction on the quality characteristics of polyester/cotton vortex yarn. Journal of Engineered Fibres and Fabrics 9(4):148-156. https://doi.org/10.1177/155892501400900418.

Lawrence C, Baqui M (1991) Effects of machine variables on the structure and properties of air-jet fasciated yarns. Textile Research Journal 61(3):123-130. https://doi.org/10.1177/004051759106100301.

Leitner H, Schwippl H (2015) Processing TENCELVR fibres. Processing of various cut staples at different delivery speed on the Rieter air-jet spinning machine using TENCELVR fibres. Rieter Machine Works Ltd Wintherthur.

Li X, Fang K, Shi L, et al (2024) Low-temperature and efficient crosslinking of lyocell knitted fabric with an eco-friendly diepoxy agent for fibrillation resistance. Cellulose 31:717–735 https://doi.org/10.1007/s10570-023-05618-6.

Mertová I, Moučková (2020) Effect of the selected machine variables on the structural characteristics of air-jet spun yarn. The Journal of The Textile Institute 111(11):1556–1566. https://doi.org/10.1080/00405000.2020.1715607.

Neckář B, Das D (2012) Theory of Structure and Mechanics of Fibrous Assemblies, Woodhead Publishing India, ISBN 9781845697914.

Neckář B, Das D (2018) Theory of Structure and Mechanics of Yarns, New Delhi, India, Woodhead Publishing India Pvt. Ltd., 1, ISBN: 978-93-85059-40-7.

Pavlović Ž, Vrljičak Z (2020) Comparing double jersey knitted fabrics made of tencel and modal yarns spun by different spinning methods. Journal of Engineered Fibres and Fabrics 15. https://doi.org/10.1177/1558925020919854.

Rieter & Textile World (2012). Spinning with an air jet. March/April 2012. Retrieved from http://www.textileworld.com/Issues/2012/March-April/Features/Spinning_With_An_Air_Jet. Accessed 25 October 2025.

Şardağ S (2019) Investigation of mechanical properties of fabric woven with Tencel/cotton blend yarns. Textile and Apparel 29(2):162-170. https://doi.org/10.32710/tekstilvekonfeksiyon.503392.

Schaeffler G (2007) *Air-jet spinning device*. US Patent Application US 2007/0125062 A1.

Shang S, Hu B, Yu C, Pei Z (2016) Effect of wrapped fibre on the tenacity of viscose vortex yarn. Indian Journal of Fibre and Textile Research 41(3):278–283.

Soe A K, Takahashi M, Nakajima M, Matsuo T, Matsumoto T (2004) Structure and properties of MVS yarns in comparison with ring yarns and open-end rotor spun yarns. Textile Research Journal 74(9):819–826. https://doi.org/10.1177/004051750407400911.

Stalder H (2014) The Rieter Manual of Spinning: Volume 6 - Alternative Spinning Systems. Rieter Machine Works Ltd. ISBN 978-3-9523173-6-5.

Tyagi GK, Sharma D (2004a) Performance and low-stress characteristics of polyester-cotton MVS yarns. Indian J Fibre Text Res; 29: 301–307.

Tyagi GK, Sharma D, Salhotra KR (2004b) Process-structure property relationship of polyester-cotton MVS yarns part I: Influence of processing variables on yarn structural parameters. Indian Journal of Fibre & Textile Research 29(4):419–428.

Vidhya MKP, Prakash C (2021) Study on single jersey knitted fabrics made from cotton/ polyester core spun yarns. Part i: thermal comfort properties. Tekstil Ve Konfeksiyon 31(4):295-305. https://doi.org/10.32710/tekstilvekonfeksiyon.906216.

Vysanska M, Mouckova E (2025) Determination of the percentage of wrapper fibres in air-jet yarn by computed tomography cross-sections. Journal of Engineered Fibres and Fabrics. 20:1-13. https://doi.org/10.1177/15589250251386536.

Zeng Y, Yu C (2003) Numerical simulation of air flow in the nozzle of an air-jet spinning machine. Textile Research Journal 73(4):350-356. https://doi.org/10.1177/004051750307300413.

Zeng Y, Yu C (2004) Numerical simulation of fibre motion in the nozzle of an air-jet spinning machine. Textile Research Journal 74(2):117-122. https://doi.org/10.1177/004051750407400206.

Zheng S, Zou Z, Shen W, Cheng L (2012) A study of the fibre distribution in yarn cross-section for vortex-spun yarn. Textile Research Journal 82(15):1579-1586. https://doi.org/10.1177/0040517511431315.

Zou Z, Cheng L, Xue W, Yu J (2008) A study of the twisted strength of the whirled airflow in Murata vortex spinning. Textil Research Journal 78:682–687.

Zou Z, Yu J, Xue W, Zhu Y, Wu J, Cheng L (2009a) Analysis of the Fibre Spatial Trajectory in Vortex Spun Yarn. Textile Research Journal 79(10):924-929 https://doi.org/10.1177/0040517508095609.

Zou Z, Yu J, Cheng L, et al (2009b) A study of generating yarn thin places of Murata vortex spinning. Textile Research Journal 79(2):129–137.

Zou Z, Zheng S, Cheng L, Xi B, Yao J (2014) Effect of Some Variables on the Fibre Packing Pattern in a Yarn Cross-section for Vortex Spun Yarn. FIBRES & TEXTILES in Eastern Europe 22(2):40-46.

Zou Z, Liu S, Zheng S, et al (2010) Numerical computation of a flow field affected by the process parameters of Murata vortex spinning. FIBRES & TEXTILES in Eastern Europe; 18(2):35–39.

Acknowledgements

Special thanks to Lucie Rozehnalová and Šárka Řezníčková for making some measurements and images and Jiří Janoušek for manufacturing yarn samples.

Statements and Declaration

Funding

The authors declare that no funds, grants, or other support were received during the preparation of this manuscript.

Competing Interests

All authors certify that they have no affiliations with or involvement in any organization or entity with any financial interest or non-financial interest in the subject matter or materials discussed in this manuscript.

The authors have no competing interests to declare that are relevant to the content of this article.

Conflicting Interests

The author(s) declare no potential conflicts of interest concerning the research, authorship, and publication of this article.

Data Availability

The data that support the findings of this study are available from the corresponding author upon reasonable request.

Ethics declaration: not applicable.

Author Contributions

All authors contributed to the conception and design of the study. Eva Moučková carried out the scientific research. Iva Mertová designed and developed the methodology, performed the measurements related to the methodology, and processed the corresponding data. Petra Jirásková performed selected yarn property measurements and analysed the obtained data. All authors contributed to the discussion and interpretation of the results. All authors commented on previous versions of the manuscript. All authors read and approved the final manuscript.